Effect of ballistic impact on Ti6Al-4V titanium alloy and 1070 carbon steel bi-layer armour panel

Citation for published version:
Shasthri, S & Kausalyah, V 2020, 'Effect of ballistic impact on Ti6Al-4V titanium alloy and 1070 carbon steel bi-layer armour panel', *International Journal of Structural Integrity*, vol. 11, no. 4, pp. 557-565.
https://doi.org/10.1108/IJSI-09-2019-0095

Digital Object Identifier (DOI):
10.1108/IJSI-09-2019-0095

Published In:
International Journal of Structural Integrity

Effect of Ballistic Impact on Ti6Al-4V Titanium Alloy and 1070 Carbon Steel Bi-Layer Armour Panel

[1] S. SHASTHRI, [2] V.KAUSALYAH,
[1] Heriot Watt University Malaysia (HWUM), [2] Universiti Teknologi Mara (UiTM)
Email: s.sivaguru@hw.ac.uk

ABSTRACT

Ballistic missile resistant impact panels have seen fair advancement over the years especially in military applications. However high cost as well as a changing materials landscape has impressed the need for a deeper understanding of impact mechanism as well as new permutations in design strategy development. Parameters such as projectile impact angle, panel impact location as well as application of multi-layer sandwich panels are not fully explored and characterised. In this work, Finite Element Method simulation methodology is used on a 25mm by 25mm plate of 3.5mm thickness, to investigate the above mentioned parameters and conditions. Solid elements using Johnson-Cook damage material models are developed. Two common impact angles 90˚ and 45˚ at centre and plate edge locations are investigated for single layer Titanium alloy and Carbon steel panels. Subsequently, a bilayer panel comprising of titanium alloy at the impact layer with the same overall plate thickness is investigated for impact at five different impact speed (ranging from 100 ms^{-1} to 500 ms^{-1}). The displacements and von Mises stresses are documented for all cases and it is shown that angular impact angles bring about greater plastic deformations as well as higher fracture likelihood compared to normal angle impact. Findings also indicate that with an addition of 1mm thick Ti-6Al-4V front bilayer, the impact resistance of the high carbon steel is significantly improved (up to twice the impact load) especially at higher impact velocities. The study documents the properties of titanium alloy- carbon steel bilayer armoured panel, which shows good promise for its implementation due to its superior performance and its cost savings potential.

Keywords: Armoured panels; Impact resistance; Bilayers panel; Ductile material;

INTRODUCTION

Research in high speed impact is pervasive in a wide range of fields ranging from industry to military applications where defensive layer versatility and effect protection are critical in the later. Armoured Fighting Vehicle (AFV) have seen much development of impact resistance research from the evolution of the first generation of tanks to the current (Ramesh 2017). Various steel alloys were used in the early generation of battle tanks as it was proven to have good resistance against impacts. 1070 carbon steel which is commonly used in the automotive industry is a common material of choice, besides the more expensive high strength steels and high hardness steels, due to its good combination of hardness, ductility and tensile strength, not to mention its relative low cost (Ramesh 2017). Later generations of AFV include titanium alloys which have seen applications in the aero-spatial, energy and biomaterial industries due to its high specific strength and fracture toughness. Excellent combinations of strength to weight ratio as well as high corrosion resistance makes titanium alloys a great material choice for armoured panels (Andrade et al. 2010).However, titanium alloys are very costly and efforts are still needed to justify performance with cost. One promising option is to consider the use of laminates.

Wang et al. (2013) studied the energy absorption of carbon fibre reinforced polymer (CFRP) laminates under high velocity impact. The CFRP laminates were impacted using a two-stage light gas gun and the energy absorption efficiency (EAE) was measured at various thickness of the plate. It was found that thin CFRP laminates have good EAE under greater impact velocities (Quaresimin et al. 2013). As metals are generally superior in impact resistance properties compared to polymers, the idea of thin laminate bilayers studied by Wang et al. (2013) holds potential in extrapolating the concept to metallic bilayers in improving the metal panels for greater resistance of high speed impact at a lower cost.

Simulation methods are proven to be a very cost effective way to investigate engineering problems. The problem of high speed impact involves dynamic analysis utilising explicit solvers and issues have arisen in the selection and correct modelling of the material relationship due to very high plasticity and rupture at very short impact time leading to spall behaviour. One particular study conducted by the department of mechanical engineering faculty of Engineering Marmara University towards the ballistic resistance of high hardness armour steels against 7.62 mm armour piercing ammunition addresses this problem (Ramesh 2017). The experiment was testing the ballistic limit of 500 HB armour steel against 7.62 mm 54R B32 API hardened steel core ammunition. The material was tested using steel and ammunition hardened steel core which was developed using the Johnson-Cook consecutive relations for both strength and failure models. The findings show that the Johnson-Cook material model for target material is capable to characterize spall behaviour during penetration.

Wang and Shi (2013) conducted an experiment to validate the Johnson-Cook plasticity and damage models using impact experiment. The experiment was conducted by analysing the dynamic response of Ti-6Al-4V under high speed ball impact at various velocities and angles. The target material was modelled base on the Johnson -Cook model that induced both plastic deformation and damage mechanism (Kistler and Waas 1998). The Johnson-Cook model for plasticity is then compared with the experimental data using foreign object damage (FOD) which shows the dent shape created by the impact and was measured in terms of the distance of dent after impact. Both the experiment and simulation show similar trend and good agreement in the crater formation at different velocities and angles. Consecutively, the Johnson-Cook model is among the most popular models used in the high velocity impact study due to its simplicity and the ease of determining the constants of the materials. The models are based on stress-strain response as a function of large strain, strain rate and the accumulation of damage and mode of failure (Rule and Jones 1998).

In high speed bullet impact against armour panels, besides material, layer thickness and simulation material model development, there are also considerations of geometry, location of impact and impact angle (Tita et al. 2008) (Gupta et al. 2008). In practical situations, projectile impacts are not always located at the centre of the armoured panels. Moreover, such high velocity impacts will frequently come at various angles of attack. Impact at various angles will contribute towards the friction and the formation of craters and dents which will lead to plastic deformation or even premature failure of the armoured panel. There is scope for research to carry out investigations into these factors as well as their interrelationship. In this work, the focus will be on the impact of a high velocity ballistic impactor at the centre and edge of the armoured panel with two selection angle of attack which are 90° and 45° (See Figure 1). The former represents standard normal impact whereas the 45° oblique angle is selected as a preliminary investigation into angular impact. The second part of the work tests the effectiveness of using thin bilayer armoured panel and comparing between conventional single layer panels of different commonly used materials for a more cost effective solution.

METHODOLOGY

A 25 by 25 mm panel with a thickness of 3.5 mm with fixed constraints along the side edges is impacted with a 6 mm diameter steel sphere at the centre. This is done for Ti-6Al-4V Titanium alloy material as well as for the 1070 carbon steel material. Figure 1(a) shows the schematic diagram of the geometry configuration of the armour panel and impacting bullet. A commercial CAE package is used as the solver as well as to carry out the model pre and post processing. For greater accuracy, modelling strategy using 3D solid brick elements were used for which acceptable mesh convergence was seen at 96440 elements. Average mesh size was approximately 0.2 mm by 0.2 mm by 0.2 mm. Dynamic explicit solver was used with a time step of 0.05s.

A baseline numerical model was developed and compared with experimental results to establish simulation model verification. This is accomplished by simulating a Ti-6Al-4V panel with centre impact at 2 impact angles, and the ensuing deflection was compared against identical experimental data from literature. Previous work (Kistler and Waas 1998, Materials Data Book 2013, Wang X et al 2013) has indicated that there is good agreement between the simulation results and the experimental data with regards to the deflection shape as well as vertical displacement values for these types of problems measured at the distance along the path of the dent, as shown in Figure 2. Upon achieving model verification, the two single panel baseline models as well as a new bilayer model (Figure 1(b)) is then investigated. The bilayer panel comprises of a 2.5 mm thick 1070 carbon steel with an additional Ti-6Al-4V 1 mm thick front panel giving a total thickness of 3.5mm. The same impact conditions as the baseline models were employed. The bilayer vs single layer panel impact simulations were carried out with five different impact velocities at 100 ms^{-1}, 200 ms^{-1}, 300 ms^{-1}, 400 ms^{-1} and 500 ms^{-1}. Two different angles of attack are used namely 90° and 45° for the centre impact whereas location of impact is also investigated, as shown in Figure 3, both at centre as well as edge for which only 90° impact angle is used. Displacement and von Mises stress response is recorded at locations on the plate measured along the line that passes through the centre point of impact.

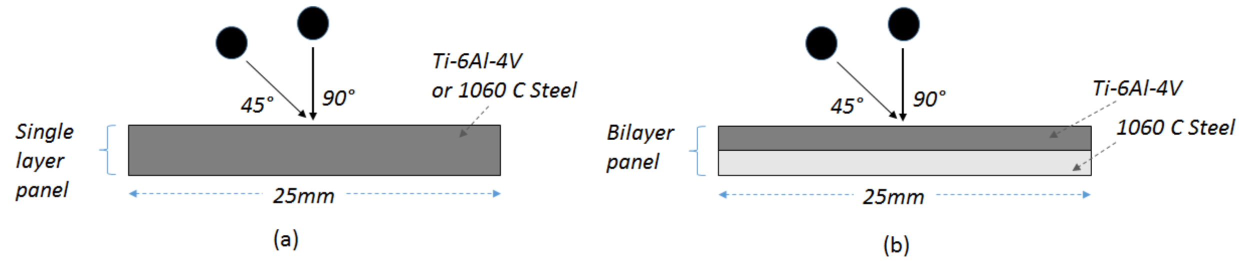

FIGURE 1. Schematic diagram of impact simulation

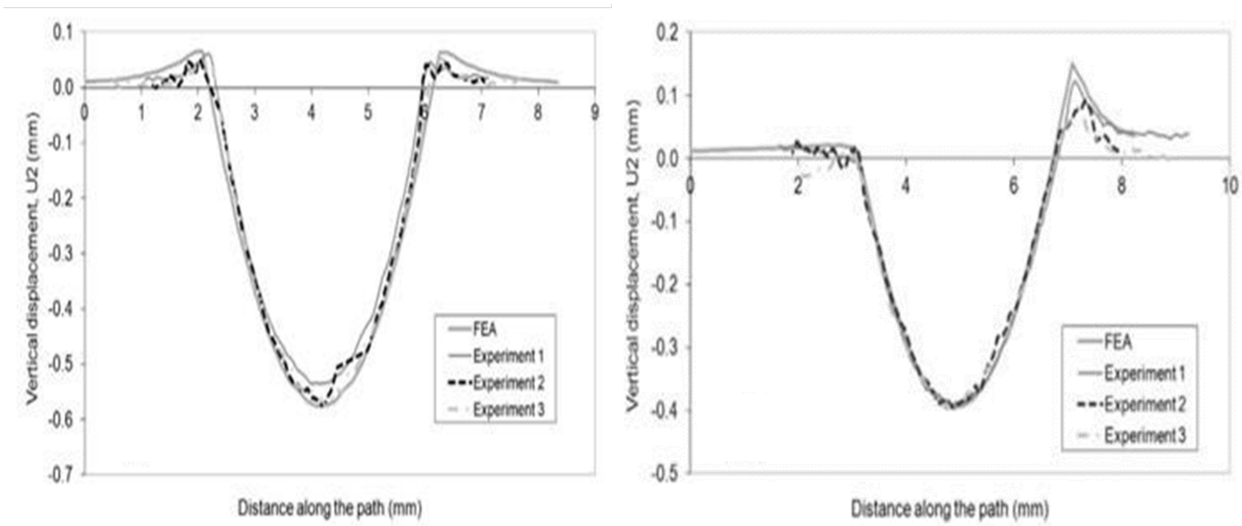

FIGURE 2. Validation of baseline model (Wang et al. 2013)

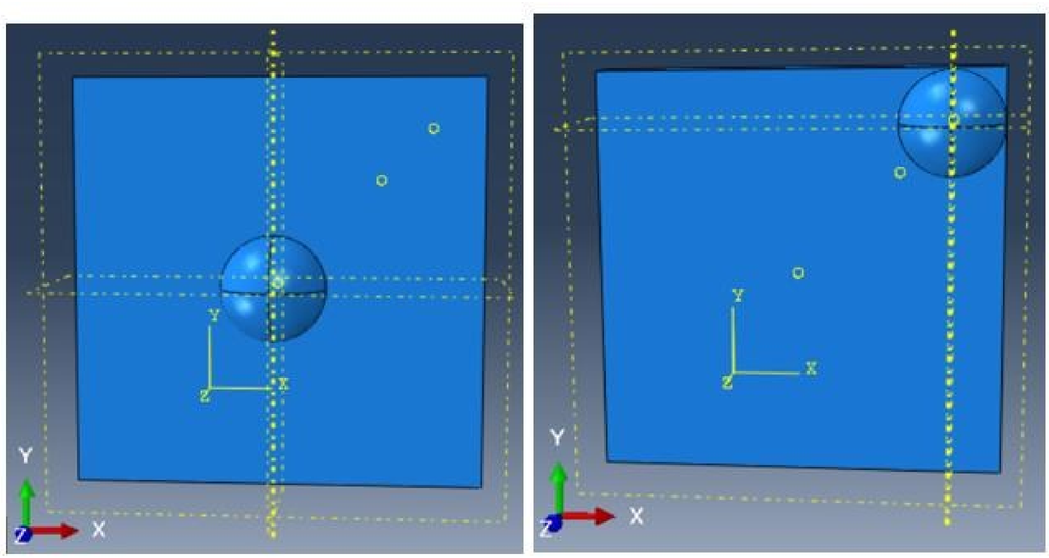

FIGURE 3. Position of the reference line for analysis

The Johnson-Cook (J-C) Damage mechanism was used as the material model for all the analysis cases as this is commonly used in impact and penetration related problems involving metals (Wang and Shi 2013). This is suitable for the simulation since the panels will experience high strain rate, large stresses as well as an increase in temperature when it undergoes dynamic impact. However, for this simulation, the adiabatic heat was not considered since the deformation and plastic strain is less than 1% (Sanaan 2013). The Johnson-Cook Damage mechanism is based on the value of the equivalent plastic strain at element integration points. Upon damage occurrence, the stiffness of the material decreases according to the specified damage evolution relationship. The damage parameter ω is defined as

$$\omega = \sum \left(\frac{\Delta \bar{\varepsilon}^{pl}}{\bar{\varepsilon}_f^{pl}} \right) \quad \ldots\ldots\ldots\ldots\ldots\ldots\ldots\ldots\ldots\ldots\ldots\ldots (1)$$

where

$\Delta \bar{\varepsilon}^{pl}$ is an increment of the equivalent plastic strain,

$\bar{\varepsilon}_f^{pl}$ is the strain at failure given as

$$\bar{\varepsilon}_f^{pl} = \left[d_1 + d_2 \exp\left(d_3 \frac{p}{q} \right) \right] \left[1 + d_4 \ln\left(\frac{\dot{\bar{\varepsilon}}^{pl}}{\dot{\varepsilon}_0} \right) \right] \left(1 + d_5 \hat{\theta} \right), \quad \ldots\ldots\ldots\ldots\ldots\ldots (2)$$

where

d_1–d_5 are failure parameters measured at or below the transition temperature

$\dot{\varepsilon}_0$ is the reference strain rate.

p/q non-dimensional ratio where p is the pressure stress and q is the von Mises stress

TABLE 1. Material Properties

Material Properties	Ti6Al-4V	1070 Carbon Steel
Density	4428 kg/m3	7800 kg/m3
Shear modulus	41.9 GPa	72 GPa
Young's modulus	109.8 GPa	190GPa
Poisson's ratio	0.31	0.29
Yield Strength	1098 MPa	500 MPa
J-C Damage constant d_1	-0.09	0.05
J-C Damage constant $d_@$	0.27	0.8
J-C Damage constant d_3	0.48	-.044
J-C Damage constant d_4	0.014	-0.046
J-C Damage constant d_5	3.87	0

(Kay G 2002, Banerjee et al 2017)

Table 1 gives the material properties used in this simulation study. The fracture energy based progressive damage can identify the damage evolution through progressively degrading the material stiffness until failure within the material's damage variable (Peirs et al. 2011). Energy dissipated of the impact is equivalent to the critical strain energy release rate, Gc. If maximum degradation is reached, deletion of element from the model occurs. This is then used as an indication of poor performance of the armoured panels against high velocity impact.

RESULTS AND DISCUSSION

TI-6AL-4V TITANIUM ALLOY MODEL

Table 2 and Figure 4 show the maximum deflection values and trends recorded at various locations relative to the centre of impact for both centre impact (90° and 45°) and edge impact (90°) at impact velocity of 200 ms^{-1} for the Ti-6Al-4V Titanium Alloy. For centre impact, simulation results show plastic deformation with a maximum value up to 0.3 mm (irrespective of attack angle) which is less than the thickness of the armoured plate (3.5 mm). For 90° impact, as expected, maximum deflection at the centre reduces incrementally at locations further away from the centre of impact. When the bullet is fired at an angle of 45°, the distribution of impact force shifts slightly toward the angle of attack as can be seen from the graph trend in Figure 3. It indicates that the maximum deflection during 90° impact is noted at the centre of the panels, which is at location 13.6 mm of the path, while the 45° maximum deflection shifts to location 10.8367 mm of the path. However, the maximum displacement is the highest (up to 0.8094 mm) when the impact is at the edge as compared with the centre impact. The distribution of the displacement is focussed on the edge of the panels and decreases as it moves further away from the edge. This indicates that the armoured panel undergoes greater plastic deformation when it is hit at the edge of the armoured panel and most likely to be exposed to failure during impact.

TABLE 2. Maximum deflection along the line at centre of impact

Distance along the line, mm	Maximum deflection at 90°, mm	Maximum deflection at 45°, mm	Maximum displacement at edge impact, mm
0	0	0	-0.80491
2.70918	-0.04225	-0.038	-0.80846
5.41836	-0.12846	-0.134	-0.77069
8.12375	-0.22289	-0.222	-0.63792
10.8367	-0.29374	-0.342	-0.45189
13.5459	-0.30167	-0.298	-0.2057
16.2551	-0.22874	-0.255	-0.09035
18.9643	-0.14014	-0.1766	-0.05637
21.6734	-0.06215	-0.0857	-0.02545
24.3826	-0.01079	-0.0176	-0.00488
25	0	0	0

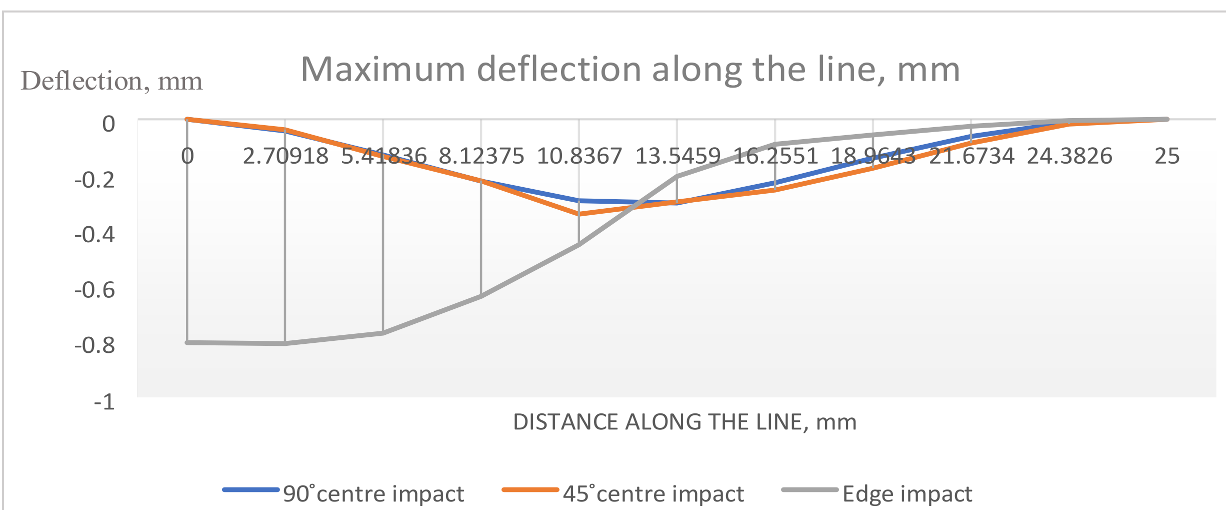

FIGURE 4. Maximum deflection graph along the line for single layer plate

Table 3 and Figure 5 shows the von Mises stress response for the same cases. When comparing between the 45° and 90° impact, the highest von Mises stress is recorded at the centre of the impact which is at the distance of 13.6

mm with stress up to 780 MPa. The plate edges also record high stresses. For the 45° centre impact, a similar trend is seen but with slightly higher magnitude of a maximum of 879 MPa. The stress plot showed higher stress concentrations at the edge following the direction of the impact. Comparing between the von Mises stress and the tensile strength of the armoured panel (1098 MPa), fracture is seen to occur at the edge of the armoured panel at the distance of 16.3 mm until 21.7 mm away from the impact point, as shown in Figure 5. This is due to plastic deformation and inertia of the armoured panel absorbing the impact energy. Therefore, the shape of the armoured panel can be a factor in establishing the fracture stress.

TABLE 3. Maximum stresses at 90° and 45° impact along the line at centre of impact

Distance along the line, mm	von Mises stress at 90° impact, MPa	von Mises stress at 45° impact, MPa	von Mises Stress at edge impact, MPa
0	736	842	117
2.70918	711	803	241
5.41836	702	761	251
8.12375	684	805	336
10.8367	677	864	694
13.5459	780	879	984
16.2551	756	832	1123
18.9643	721	779	1126
21.6734	665	786	1106
24.3826	696	799	1068
25	732	805	965

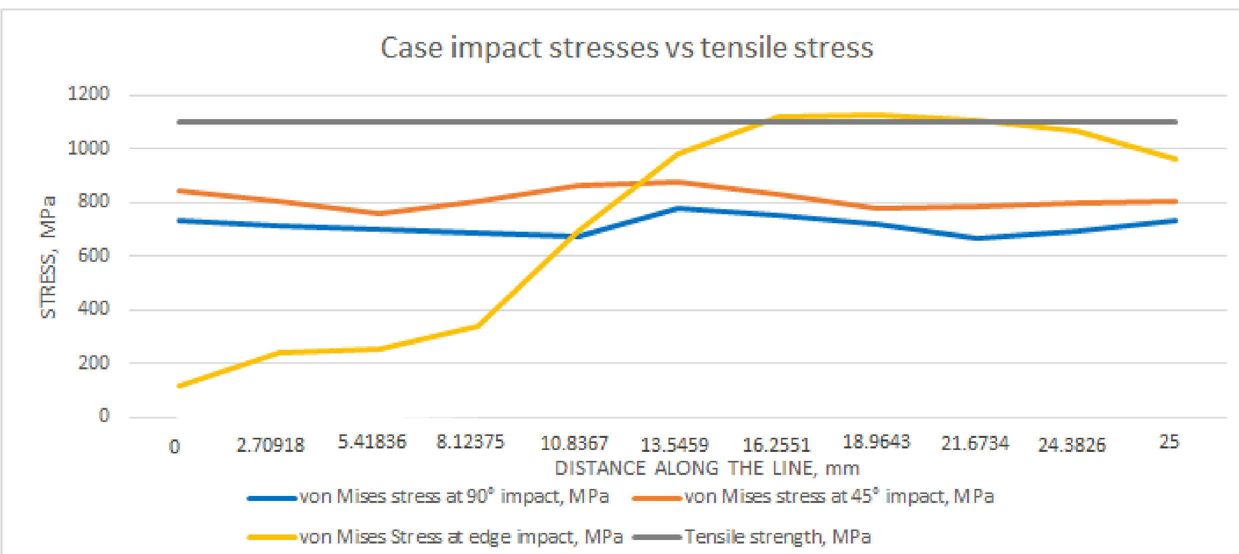

FIGURE 5. Case impact stresses vs material tensile stress

CARBON STEEL PANEL AND BILAYER PANEL MODELS

Table 4 and Figure 6 show the comparison of impact at different velocities on single layer (1070 carbon steel) plate and on bilayer (1070 carbon steel plate with a Ti-6Al-4V outer panel). For the former, the results show that fracture occurs at 180 ms^{-1} impact velocity. From this velocity onwards, the stress exceeds the tensile strength of the 1070 carbon steel plate. Formation of bulk is noted at the impact location along with the fracture and spall behaviour of the 1070 carbon steel at the back of the plate. This indicates possibility of broken detached parts which will form a hole at the centre of the armoured panel. However, the results indicate that with an addition of 1mm thick Ti-6Al-4V front bilayer, the failure of the high carbon steel is greatly reduced especially at higher velocities. Failure is shown to only occur at a velocity of 387 ms^{-1}. The Ti-6Al-4V layer acts as a medium to absorb the impact energy away from the more vulnerable high carbon steel layer, thus considerably improving impact resistance against bullet strikes.

TABLE 4. Stress distribution at various impact velocities between 1070 carbon steel and bilayer panel

Velocity, m/s	100	200	300	400	500
1070 carbon steel von Misses stress, MPa	14	373	564	795	1340
Bilayer von Mises stress, MPa	18	112	233	326	446
Tensile yield strength, MPa	304	304	304	304	304

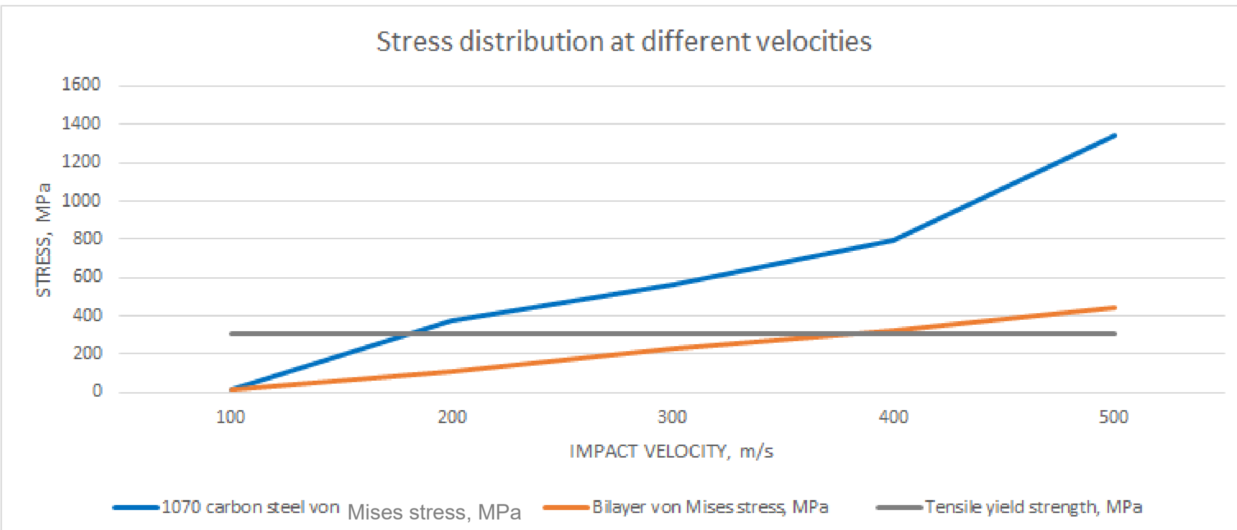

FIGURE 6. Stress distribution at different velocities for bilayer and 1070 carbon steel panel

CONCLUSION

Ti6-Al-4V titanium alloy and 1070 carbon steel armour panels as well as a bilayer armour panel were subjected to different high velocity ballistic impact was studied at two impact angles and impact locations against stress and deflection. Simulation results show that when a 1 mm thick Ti-6Al-4V is placed at the front of the 2.5 mm thick steel plate as a bilayer armour, the panel is able to withstand twice the impact due to a ballistic bullet as compared to a single layer 1070 carbon steel plate with the same thickness. Simulation was also carried out between the centre of the plate and the edge of the plate impact point. For the impact at various places in simulation one, the comparison was made between the centre of the plate and the edge of the plate. The results show that centre impact give an even distribution of stress. For the edge impact, failure was seen to occur. Additionally, investigations on non- perpendicular impact angle (45°) show higher plastic deformation. The study documents the properties of titanium alloy-carbon steel bilayer armoured panel, which shows good promise for its implementation due to its superior performance and possible cost reduction. A more detailed parametric study and cost analysis is recommended to further corroborate these findings towards establishing design parameters.

REFERENCES

Andrade, A. Morcelli A. and Lobo. R., *"Deformation and fracture of alpha/beta titanium alloy*", Revista Matéria, (2010), v. 15, n. 2, pp. 364-370. Available at: http://www.scielo.br/pdf/rmat/v15n2/38.pdf (Accessed: 15 January 2018)

Banerjee A., Dhar S., Acharyya S., Datta D., Nayak N., *"Numerical Simulation of Ballistic Impact ofArmour Steel Plate by Typical Armour Piercing Projectile",* Procedia Engineering, (2017), 173, pp. 347-354. doi.org/10.1016/j.proeng.2016.12.028

Gupta, N. K., Iqbal, M. A. and Sekhon, G. S., "*Effect of projectile nose shape, impact velocity and target thickness on the deformation behavior of layered plates"*, International Journal of Impact Engineering, (2008) 35(1), pp. 37–60. doi: 10.1016/j.ijimpeng.2006.11.004.

Kistler, L. S. and Waas, A. M., *"Impact response of cylindrically curved laminates including a large deformation scaling study"*, International Journal of Impact Engineering, (1998), 21(1–2), pp. 61–75. doi:10.1016/S0734-743X(97)00031-6.

Materials Data Book 2013. http://www-mdp.eng.cam.ac.uk/web/library/enginfo/cueddatabooks/materials.pdf (Accessed: 17 June 2018)

Peirs, J., Verleysen P, Van Paepegem W, and Degrieck J., "*Determining the stress-strain behaviour at large strains from high strain rate tensile and shear experiments"*, International Journal of Impact Engineering, (2011), 38(5), pp. 406–415. doi: 10.1016/j.ijimpeng.2011.01.004.

Quaresimin, M., Ricotta M., Martello L. and Mian S., *"Energy absorption in composite laminates under impact loading"*, Composites Part B: Engineering, (2013), 44(1), pp. 133–140. doi: 10.1016/j.compositesb.2012.06.020.

Ramesh, S. *"Armoured fighting vehicle - Future perspective"*, Defence Science Journal, (2017), pp. 341– 342. doi: 10.14429/dsj.67.11544.

Rule, W.K. and Jones, S.E., *"A revised form for the Johnson–Cook strength model"*. International Journal of Impact Engineering, (1998), 21(8), pp.609-624.

Sanaan H. Khan, *"'Johnson-Cook Empirical Models"*, www.scribd.com , (2013)., https://www.scribd.com/doc/130548707/Johnson-Cook-Empirical-Models (Accessed: 20 July 2018)

Tita, V., de Carvalho, J. and Vandepitte, D. *"Failure analysis of low velocity impact on thin composite laminates: Experimental and numerical approaches"*, Composite Structures, (2008), 83(4), pp. 413–428. doi:10.1016/j.compstruct.2007.06.003.

Wang, B., Xiong J., Wang X., Feng J., *"Energy absorption efficiency of carbon fiber reinforced polymer laminates under high velocity impact"*, Materials & Design, (2013), 50, pp. 140–148. doi:10.1016/j.matdes.2013.01.046.

Wang, X. and Shi, J., *"Validation of Johnson-Cook plasticity and damage model using impact experiment"*, International Journal of Impact Engineering, (2013), 60, pp. 67–75. doi:10.1016/j.ijimpeng.2013.04.010.

Kay, G., *"Failure Modeling of Titanium-6Al-4V and 2024-T3 Aluminum with the Johnson-Cook Material Model",* U.S. Department of Energy Office of Scientific and Technical Information: Technical Report, (2002), doi:10.2172/15006359.